Interaction of NH3 with Brønsted acid sites in different cages of zeolite Y as studied by 1H MAS NMR

Interaction of NH_3 with Brønsted Acid Sites in Different Cages of Zeolite Y As Studied by ^1H MAS NMR

W. P. J. H. Jacobs,*,† J. W. de Haan,‡ L. J. M. van de Ven,‡ and R. A. van Santen†

Schuit Institute of Catalysis, Laboratory of Inorganic Chemistry and Catalysis, and Laboratory of Instrumental Analysis, Eindhoven University of Technology, P.O. Box 513, 5600 MB Eindhoven, The Netherlands

*Received: March 18, 1993; In Final Form: June 29, 1993**

Ammonia adsorption onto acidic Y zeolites is studied with ^1H MAS NMR (at 295–320 K). The influence of the amount of adsorbed ammonia is investigated in the presence of sodium or cesium as exchangeable cations and for different framework compositions (Si/Al = 2.4–12). The Brønsted sites in unloaded or partially loaded zeolites are observed near δ = 3.9 for protons in supercages and near δ = 4.6 for protons in sodalite cages. Ammonium ions under condition of no proton-exchange resonate at δ = 8.1. These species are detected as such only in the sodalite cages. In the supercages, a signal at δ = 6.9 is observed, which is ascribed to an exchange involving NH_4^+ (δ = 8.1), H^+ (δ = 3.9), and NH_3 (δ = 0.8). Furthermore, in the sodalite cages, a signal at δ = 6.5 is observed, which is ascribed to an exchange involving NH_4^+ (δ = 8.1), H^+ (δ = 4.6), and NH_3 (δ = 0.8), but with different relative residence times. Additionally, ammonium–ammonia signals are found at δ = 5.3–5.9 and at a position determined by the NH_3/NH_4^+ ratio in the zeolite (δ = 7–1). For the ammonium–ammonia species proton-exchange between ammonium and ammonia is fast compared to the time scale of the NMR experiment. For at least two ammonium species proton-exchange with the Brønsted protons is fast, and consequently the lines are shifted to δ = 6.9 and 6.5. This implies that ammonium ions observed at δ = 8.1 have the lowest basicity and the ammonium ions at δ = 6.5 have the highest basicity. However, for the temperature range used, ammonia reacts statistically with the Brønsted sites of different acid strength.

Introduction

The proton form of zeolite Y is used as a catalyst in hydrocarbon processing. This solid acid is usually obtained from the ammonium-exchanged form, after desorbing ammonia and water at elevated temperatures. Ammonia adsorption onto the proton form or the reverse process, ammonia desorption at elevated temperatures, is used to characterize the acidity of the solid acid.[1] This can be done, e.g., with temperature programmed desorption (TPD) techniques or with microcalorimetric measurements. In order to understand the experimentally obtained results at an atomic level, quantum chemical calculations are performed.[2-7] From these calculations information is obtained about the geometry of the Brønsted sites in terms of bond lengths and bond angles. Further, the energies involved in transferring the proton to the ammonia molecule are calculated, and the geometry of the ammonium ion with respect to the lattice is predicted. So, ammonia adsorption onto the zeolitic structure is an interesting subject, both for experimental and for theoretical studies of zeolite acidity.

Spectroscopic techniques are extensively used to study these phenomena. With infrared spectroscopy two bands are observed for zeolite Y, which are due to the hydroxyl stretching modes of different Brønsted sites.[8] The high-frequency band near 3645 cm^{-1} (HF-OH) is assigned to the hydroxyl groups pointing into the supercages, involving the O_1 atoms (see Figure 1). The hydrogen atoms at O_2 and O_3 in the sodalite cages cause the low-frequency band near 3550 cm^{-1} (LF-OH). Both infrared bands decrease in intensity after adsorption of ammonia, and the formation of ammonium ions is shown by the appearance of the N–H deformation modes of ammonium ions near 1450 and 1670 cm^{-1} [9] and also by the ammonium lattice vibrations near 160 cm^{-1}.[10-12] From far-infrared experiments it was concluded that the ammonium ions can be located at different cation sites, e.g., sites I′, II, and III (see Figure 1).[12]

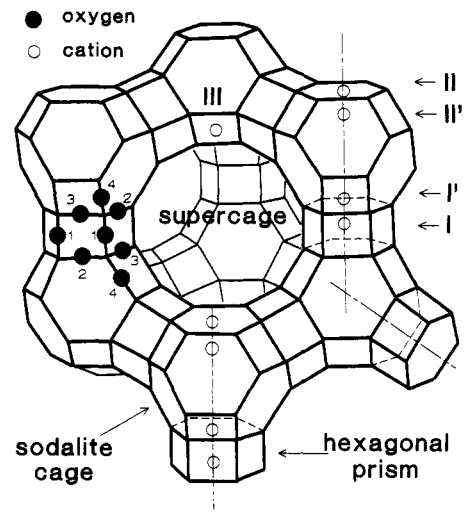

Figure 1. Faujasite structure. The different oxygen atoms are indicated by the numbers 1–4. The different cation positions are indicated by Roman numerals.

Inelastic neutron scattering (INS) spectroscopy is especially sensitive toward vibrational, librational, or rotational motions of hydrogen atoms. Results for zeolite Y obtained with this technique indicated that the librational motions of ammonium ions in the sodalite cage are more restricted than for those located in the supercages.[13] The time scale of these librations are in the order of a few picoseconds as can be concluded from quasi-elastic neutron scattering (QENS) experiments.[14,15]

^1H MAS NMR is nowadays widely used in the characterization of acidic catalysts. In the past the Brønsted sites in zeolite Y have been extensively studied with this technique.[16-23] These studies have resulted in the assignment of different signals for zeolites Y: (a) δ = 1.8–2.3 caused by terminal Si–OH groups, (b) δ = 3.8–4.4 caused by the acidic protons pointing into the supercages, (c) near δ = 5.2 caused by protons in the sodalite cages, (d) δ = 6.5–7.0 due to ammonium ions, and (e) δ = 2.6–3.6

† Laboratory of Inorganic Chemistry and Catalysis.
‡ Laboratory of Instrumental Analysis.
* Abstract published in *Advance ACS Abstracts*, September 1, 1993.

0022-3654/93/2097-10394$04.00/0

TABLE I: Samples and Compositions, Loadings with Ammonia, and Observed NMR Lines at a MAS Frequency of 9 kHz

samples		loading of	chemical shift (ppm) (signals: (sh) shoulder, (w) weak, (vw) very weak)							
			O–H				N–H			
no.	composition[a]	NH_3/unit cell								
1	$Na_{43}(NH_4)_8$–Y (Si/Al = 2.8)	0.0	4.5[w,sh]	3.82		1.9[w]				
		3.6	4.5[w,sh]	3.80		1.9[w]		7.4[sh]	6.85	
		31				1.0[w]			5.27[vw]	3.27
		51				1.0[w]			5.36[vw]	2.54
2	$Na_{28}(NH_4)_{23}$–Y (Si/Al = 2.8)	0.0	4.7[sh]	3.90		2.0[w]				
		3.6	4.7[sh]	3.86		2.0[w]		7.4[sh]	6.94	
		10.2	4.5[sh]	3.86		2.0[w]		7.5[sh]	6.95	5.2[sh]
		51				1.0[w]				5.23 4.94
		66				1.0[w]			6.57[vw]	5.25 3.92
3	$(NH_4)_{51}$–Y (Si/Al = 2.8)	0.0	4.5[sh]	3.95		2.0[w]				
		3.6	4.5[sh]	3.96		2.0[w]			6.89	
		10.2	4.6[sh]	3.96		2.0[w]		7.9[sh]	6.88	
		51						7.8[sh]	6.47	5.4[sh]
		66						7.86	6.43	5.86
		87					8.0		6.48	5.2[sh] 4.81
		102					8.1		6.53	5.4[sh] 4.3
4	$Na_9(NH_4)_{47}$–Y (Si/Al = 2.4)	0.0	4.6[sh]	3.92		2.0[w]				
		3.9	4.6[sh]	3.89		2.0[w]		7.5[sh]	6.99	
		11.2	4.6[sh]	3.85		2.0[w]		7.5[sh]	7.04	
		95					8.1		6.47	5.20 4.17
5	$Na_3Cs_{35}(NH_4)_{18}$–Y (Si/Al = 2.4)	0.0	4.67	3.44		1.7[w]				
		4.5	4.72			1.6[w]	8.12	7.4[sh]		
		9.7	4.7			1.7[w]	8.15	7.13		
		32				1.6[w]	8.12		5.92	3.23
		64					8.13		5.89	2.21
6	Na_{51}–Y (Si/Al = 2.8)	5								0.78
		26								0.78
7	NH_4–Y (Si/Al = 5)	0.0	4.6[sh]	4.06	2.9[sh]	1.9[sh]				
		3.0	4.6[sh]	4.06	2.9[sh]	1.9[sh]			6.80	
		excess[b]			2.7			8.0[sh]	6.85	5.46
8	NH_4–Y (Si/Al = 12)	excess[b]			2.9	2.1			6.62	5.49

[a] According to chemical analysis and ^{29}Si MAS NMR. [b] Excess ammonia adsorbed at room temperature onto the proton form, followed by evacuation at room temperature.

due to hydroxyl groups of extralattice aluminium derivatives. When excess ammonia is adsorbed compared to the acidic sites in the zeolites, additional signals can be found near $\delta = 5.3$ and at a position determined by the loading with ammonia (δ = 7–0).[20-21] These signals are due to ammonium ions in fast proton exchange with ammonia. Recently, the spinning sidebands belonging to the Brønsted sites have been studied and interpreted in terms of dipolar interactions between ^1H and ^{27}Al nuclei. In this way the H–Al distances and the chemical shift anisotropies of the acidic hydroxyls are calculated.[24-26] The interaction of ammonia with Brønsted sites has been studied for zeolite rho by Vega and co-workers.[27] They showed, using ^{29}Si (CP) MAS NMR, that for the anhydrous zeolites the acidic protons and the ammonium ions are more rigidly bonded to the lattice than in the hydrated zeolites. Whereas in the anhydrous protic sample the ^1H–^{27}Al dipolar interactions are dominant, in the samples containing anhydrous ammonium the ^1H–^1H dipolar interactions in the same ion are of main importance.

Michel and co-workers[28,29] used conventional Fourier transform ^{15}N NMR to study the adsorption of ammonia onto zeolites. More recently, Earl and co-workers[30] studied the adsorption of ammonia onto zeolite Y using ^{15}N (CP) MAS NMR. They observed two different ammonium species with different mobilities. Chemical exchange or isotropic diffusion are so slow for these species that cross-polarization of ^{15}N with ^1H is possible. At high loadings with ammonia the ammonium ions interact with the ammonia molecules via hydrogen bonding, giving rise to additional features in the ^{15}N MAS NMR spectra. The excessive ammonia molecules in the zeolite are quite mobile, and they give rise to a broad chemical shift dispersion.

In this work we will use ^1H MAS NMR to study the interactions of ammonia and acid sites in the different cavities of zeolite Y, with the aim of gathering additional information regarding the interaction of the acid sites with probe molecules and the relative accessibilities of the different types of cages. More in particular we will pay attention to the partition of ammonia over different sites at low loadings and the possibly different behavior of ammonia when forced predominantly into one of the cages. Solvation is one of the factors which determine the acid strength. The solvation of the ammonium ions by the faujasite lattice will be briefly mentioned.

Experimental Section

The samples used are listed in Table I. Samples 1 and 2 were obtained by exchanging 18 g of sample 6 (Na_{51}–Y: Akzo PA42611B, Si/Al = 2.8) at room temperature in 900 mL of 0.1 M nitrate solutions, containing ammonium and sodium ions in the ratios 0.32:1 and 4.3:1, respectively. The completely exchanged sample 3 was obtained after 9-fold exchange with 1 M solutions of NH_4NO_3 at 353 K. Sample 5 was obtained after 4-fold exchange at 353 K of sample 4 (Linde LZ-Y62, Si/Al = 2.4) in 1 M solutions of NH_4NO_3, followed by 3-fold exchange at room temperature in 0.3 M solutions of CsCl. Two dealuminated Y zeolites (samples 7 and 8) were prepared by dealuminating Na_{51}–Y with $SiCl_4$ at 523 K for 15 or 60 min.[31-34] After being washed with demineralized water, the samples were converted to the ammonium forms by 4-fold exchange at 353 K in 2 M solutions of NH_4NO_3. The compositions of the samples as listed in Table I are obtained from elemental analyses on sodium, silicon, aluminium, and cesium. The Si/Al rations of the framework were determined from ^{29}Si MAS NMR experiments. According to X-ray diffraction (XRD), all samples were highly crystalline and have similar crystallite sizes (approximately 32 nm).

Approximately 200 mg of zeolite was transferred to glass ampules and heated at a rate of 1°/min to 673 K in vacuo. After

being degassed for 3 h, the samples were cooled to room temperature. The pressure was now less than 10^{-4} Pa. Anhydrous ammonia (UCAR, 99.997% purity) was subsequently adsorbed on part of the samples; the amount adsorbed was determined volumetrically. Coverages with ammonia ranging between 0.07 and 6.4 times the number of Brønsted sites were applied. Finally, the ampules were sealed. The samples were transferred from the ampules to 4-mm ZrO_2 MAS rotors of standard Bruker design under an inert nitrogen atmosphere and sealed with the spinner caps. Duration experiments indicated that no spectral changes occurred after several days, indicating that water uptake or ammonia desorption was negligible. The treatment of the samples did not result in severe structural damages, since the ^1H MAS NMR experiments revealed only very weak signals due to silanol groups or hydroxyl groups of extralattice aluminium derivatives for the nondealuminated zeolites. This is further supported by ^{27}Al MAS NMR experiments, which were performed using the samples before treatment and after readsorption of excessive amounts of ammonia. These spectra were recorded on a Bruker MSL 400 spectrometer by co-adding 1000 free induction decays (FID's) using single 25° pulses with repetition times t_r = 1 s at a sample spinning frequency of 10 kHz. For the nondealuminated zeolites in all cases a strong signal due to tetrahedrally coordinated aluminium was observed, whereas the contribution due to octahedrally coordinated aluminium was less than 0.5%. In the dealuminated samples the amount of octahedrally coordinated aluminium was approximately 5–10%. After re-adsorption of ammonia a slightly lower amount was found. This may be due to the heating procedures used.

The ^1H MAS NMR spectra were obtained at 300 MHz (7.0 T) on a Bruker CXP 300 spectrometer or at 400 MHz (9.4 T) on a Bruker MSL 400 spectrometer, both with a standard double-air bearing MAS probe. Experiments were carried out at 295 and 320 K. Spectra were obtained for stationary samples and for samples spinning at frequencies from 1 to 9 kHz. Sixteen to forty FID's were accumulated by using single 50° pulses (t_p = 1 μs) with repetition time t_r = 60 s and spectral width SW = 40 kHz. For samples saturated with ammonia, shorter repetition times (t_r = 5 s) could be used.

Infrared spectra of the zeolites in the proton forms were recorded in transmission mode on a Bruker IFS 113v FTIR spectrometer equipped with a heatable vacuum cell. Self-supported discs were used for the measurements. The samples were pretreated in the cell for 1 h at 723 K before the room temperature spectra were recorded.

Results and Discussion

Brønsted Signals. In Table I the observed NMR lines for all experiments are summarized. After samples 1–4 were heated, a NMR signal near δ = 3.9 is observed (Figures 2–4). With increasing proton concentration of the samples, a shoulder near δ = 4.6 develops. For sample 5 (Figure 4) a signal near δ = 4.7, with a shoulder at δ = 3.4, is observed. The intensities for the various signals correlate with the intensities for the infrared stretching modes of the Brønsted sites (Figure 5). At low proton concentration only the high-frequency hydroxyl (HF-OH) band is observed, and only at higher proton concentrations the low-frequency hydroxyl (LF-OH) band develops. Sample 5 shows mainly the LF-OH band since the large cesium ions cannot penetrate into the sodalite cages,[35] whereas the ammonium ions, which produce the acidic protons, can. So the signal near δ = 3.9 corresponds to the infrared HF-OH band, which is related to protons bonded to O_1 and pointing into the supercages.[8,19] The signal near δ = 4.7 corresponds to the infrared LF-OH band, which is related to protons located in the sodalite cages.[8,19] These protons are bonded to O_3 or O_2. The protons at O_3 are located near the six rings of the hexagonal prisms. The others, localized at O_2, point into the six-ring window between the sodalite cage and the supercage.[36] The protons on O_2 and O_3 both have two close oxygen neighbors at 2.6 Å in the same six ring.[36,37] Due to the presence of these oxygen atoms, the infrared stretching mode is shifted to lower wavenumbers and the NMR line is observed at lower field. For the dealuminated samples (see Table I), the band maximum (δ = 4.0) is slightly shifted to lower field. This is in agreement with the results obtained by Freude and co-workers[19], who also found a shift to lower field with increasing Si/Al ratio. Similar to the nondealuminated zeolites, a shoulder is observed at δ = 4.6, which becomes better resolved by increasing the MAS frequency from 9 to 14 kHz. Additionally, only for the dealuminated zeolites a broad but low signal near δ = 2.7 is observed due to lattice imperfections (e.g., hydroxyl groups at extraframework aluminium). These protons are non-acidic, since they do not react with ammonia. Brunner[22,23] has investigated the line broadening mechanisms for the lines due to the Brønsted sites in the ^1H MAS NMR spectra. It was concluded that at high spinning rates (more than ca. 10 kHz) and at fields from 7.0 to 11.7 T the main contribution comes from the dispersion

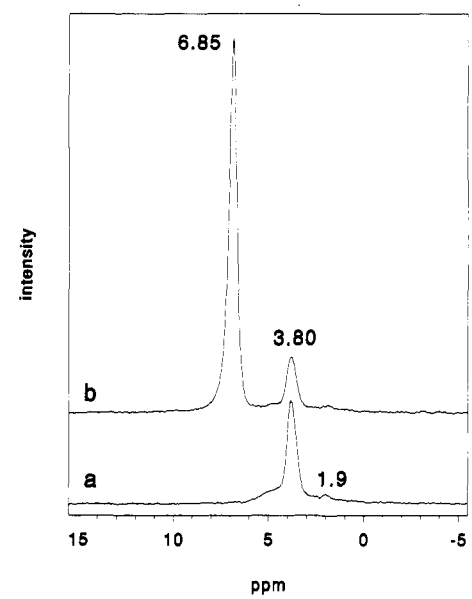

Figure 2. Room temperature ^1H MAS NMR spectrum (at 9.4 T) of sample 1 at a MAS frequency of 9 kHz: (a) unloaded sample; (b) 3.6 molecules of NH_3 adsorbed/unit cell.

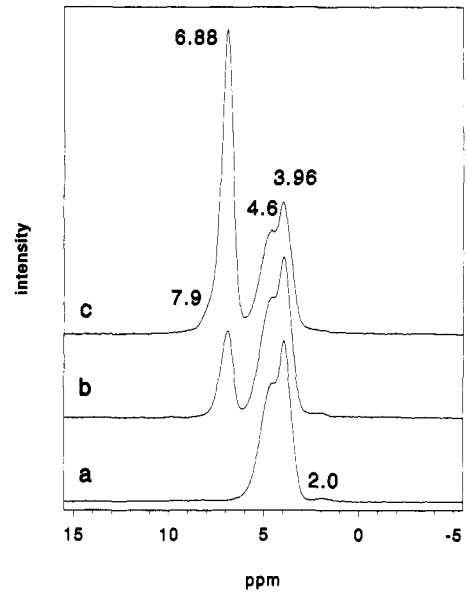

Figure 3. Room temperature ^1H MAS NMR spectrum (at 9.4 T) of sample 3 at a MAS frequency of 9 kHz: (a) unloaded sample; (b) 3.6 molecules of NH_3 adsorbed/unit cell; (c) 10.2 molecules of NH_3 adsorbed/unit cell.

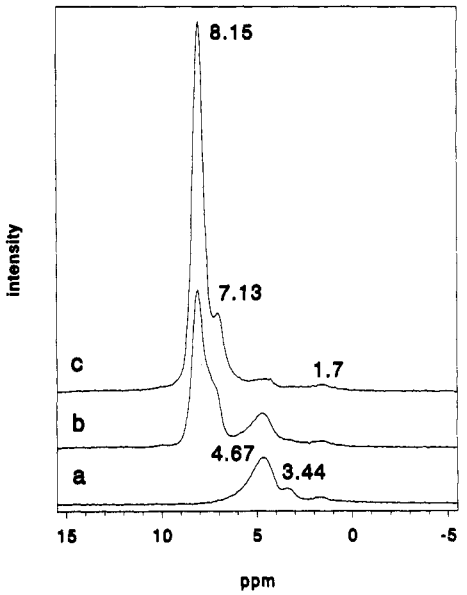

Figure 4. Room temperature ^1H MAS NMR spectrum (at 9.4 T) of sample 5 at a MAS frequency of 9 kHz: (a) unloaded sample; (b) 4.5 molecules of NH_3 adsorbed/unit cell; (c) 9.7 molecules of NH_3 adsorbed/unit cell.

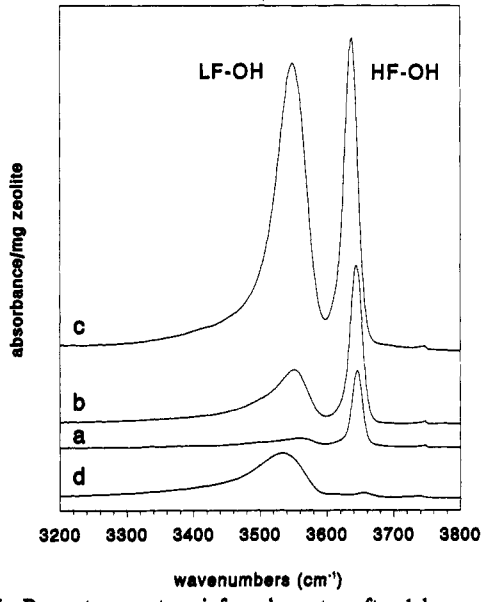

Figure 5. Room temperature infrared spectra after 1-h evacuation at 723 K of sample 1 (a), sample 2 (b), sample 3 (c), and sample 5 (d).

of the isotropic chemical shifts, which was estimated at 0.8 ppm for protons at O_1 and at 1 ppm for protons at O_2 or O_3.

When small amounts of ammonia are adsorbed (up to 12 ammonia molecules/unit cell), so that not all acidic sites have reacted, we could not observe any preferential reaction of the different types of acidic protons with ammonia (Figures 2–4). The decreases in intensities of the maximum at δ = 3.9 and of the shoulder at δ = 4.6 are the same within the experimental error. Freude and co-workers[19] found that pyridine interacts preferentially with the acidic protons in the supercages, responsible for the line at δ = 3.9. Infrared experiments showed that carbon monoxide also reacts preferentially with the acidic protons in the supercages.[38] The ammonia molecule is much smaller than pyridine and can penetrate the zeolite six rings and hence react with the Brønsted sites in the sodalite cages. Ammonia is a much stronger base than carbon monoxide. So for ammonia adsorption at room temperature the energy gain is mainly determined by the protonation energy of the ammonia molecule, whereas differences in acidity of the Brønsted sites are smaller and of minor importance. The interaction energy of carbon monoxide with

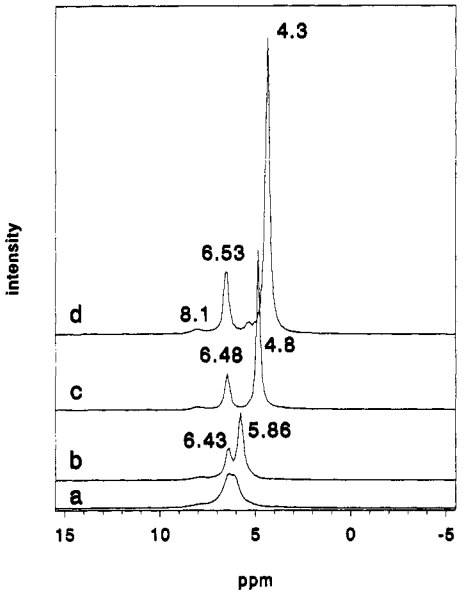

Figure 6. Room temperature ^1H MAS NMR spectrum (at 7.0 T) of sample 3 at a MAS frequency of 9 kHz and different loadings with NH_3: (a) 51 molecules of NH_3/unit cell; (b) 66 molecules of NH_3/unit cell; (c) 87 molecules of NH_3/unit cell; (d) 102 molecules of NH_3/unit cell.

the Brønsted sites is much weaker, and now differences in acid strength of the various sites become important. Since the protons at O_2 and O_3 (δ = 4.6, LF-OH infrared band) have two close oxygen neighbors at 2.6 Å,[36,37] this interaction is probably energetically favorable enough to prevent adsorption of carbon monoxide at these sites. On the other hand, Hoffmann and co-workers[39] concluded from temperature programmed desorption experiments that the hydroxyls in the supercages are the most acidic. However, these results are obtained at temperatures exceeding 450 K. At low temperature the adsorbed ammonia has probably reacted statistically with the available acidic sites, whereas at high temperatures equilibrium is obtained between sites with different acidic strengths.

Ammonium Signals. After adsorption of small amounts of ammonia an NMR signal due to ammonium ions is observed at δ = 6.9 for samples 1–4. For sample 3 this signal has a weak shoulder at lower field. At low loadings with ammonia this shoulder is observed near δ = 7.0–7.5. At excess loadings (Figures 6–8) all available acidic sites are covered with ammonia. The shoulder for sample 3 develops into a weak signal, which is shifted up to δ = 8.1 (Figure 6). The intensity of this signal corresponds to only a few ammonium ions per unit cell.

At low loadings for sample 5 a strong line is observed at δ = 8.1, with a small shoulder near δ = 7.1 (Figure 4). At excess loadings the shoulder has disappeared (Figure 8). Also, we observe now that with increasing loading the intensity for the line at δ = 8.1 decreases from approximately 18 ammonium ions/unit cell (which is the amount expected at saturation of all acidic sites) to approximately 3 ammonium ions/unit cell for the highest loading applied onto this sample.

For the samples containing no or only a few residual sodium cations (samples 3 and 4) the line previously observed at δ = 6.9 is shifted to δ = 6.5 at excess loadings and has then a much smaller line width (see also Figures 9 and 10). For sample 3 this line corresponds to approximately 16 ammonium ions/unit cell for bulk NH_3/NH_4^+ ratios between 0.3 and 1.0. (In the calculations of the NH_3/NH_4^+ ratios we assume that each Brønsted site reacts with an ammonia molecule under the formation of an ammonium ion.) For sample 4 this signal corresponds to approximately 5 ammonium ions/unit cell at a bulk NH_3/NH_4^+ ratio of 1.0 (Figure 10). Hence, the presence of this line is related to the degree of ammonium exchange of the samples. When the sodium content is moderate, the residual

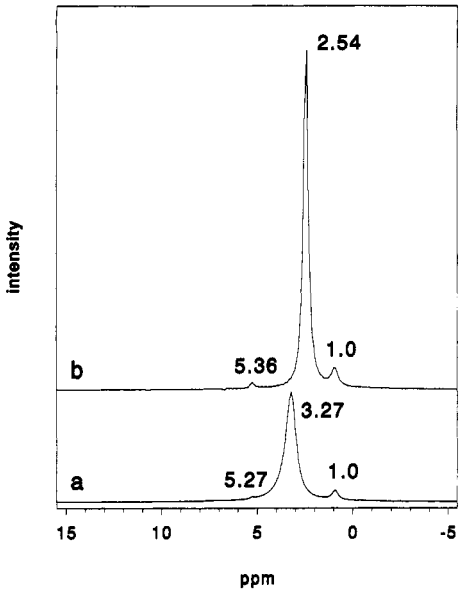

Figure 7. Room temperature ^1H MAS NMR spectrum (at 7.0 T) of sample 1 at a MAS frequency of 9 kHz and different loadings with NH_3: (a) 31 molecules of NH_3/unit cell; (b) 51 molecules of NH_3/unit cell.

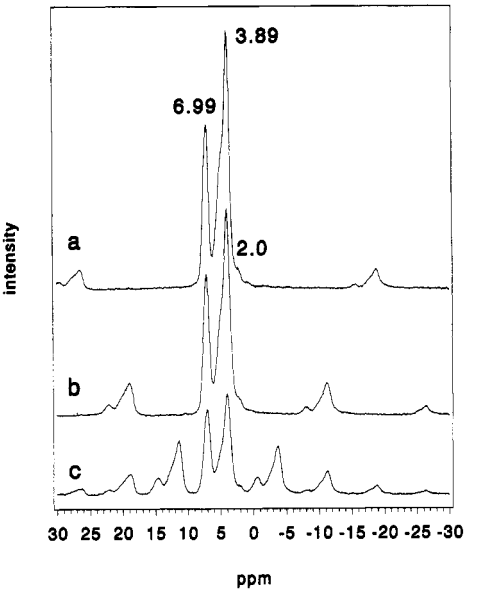

Figure 9. Room temperature ^1H MAS NMR spectrum (at 9.4 T) of sample 4 loaded with 3.9 molecules of NH_3/unit cell obtained at different MAS frequencies: (a) 9 kHz; (b) 6 kHz, (c) 3 kHz.

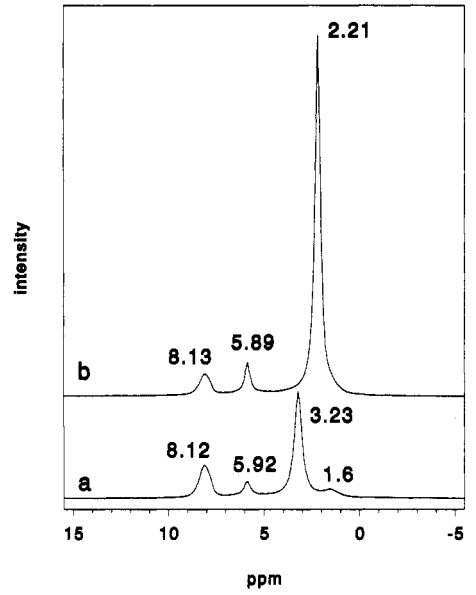

Figure 8. Room temperature ^1H MAS NMR spectrum (at 7.0 T) of sample 5 at a MAS frequency of 9 kHz and different loadings with NH_3: (a) 32 molecules of NH_3/unit cell; (b) 64 molecules of NH_3/unit cell.

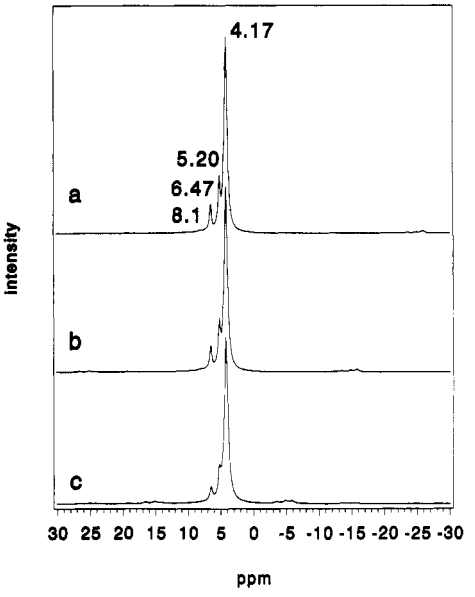

Figure 10. Room temperature ^1H MAS NMR spectrum (at 7.0 T) of sample 4 loaded with 95 molecules of NH_3/unit cell obtained at different MAS frequencies: (a) 9 kHz; (b) 6 kHz, (c) 3 kHz.

sodium cations are located at sites I′ in the sodalite cages, and some sodium cations remain at sites II in the supercages after the ammonium exchange.[40] At increasing degrees of ammonium exchange these residual sodium cations will gradually be replaced by ammonium ions in the sodalite cages at sites II′ or I′.[41] For cesium-exchanged sample 5, which contains ammonium ions mainly located in the sodalite cages, the line at $\delta = 6.5$ is absent. The cesium ions (35 per unit cell) are located at sites II and III,[40] thus preventing the nearby cation sites (especially sites II′) from being occupied by ammonium ions. So we prefer to attribute the line at $\delta = 6.5$ to ammonium ions at site II′. These findings are different from those obtained by Ozin and co-workers.[12] They proposed that ammonium ions in the sodalite cages are located at site I′ only.

When the residual sodium content is lower, the bulk NH_3/NH_4^+ ratio will be smaller at a certain loading with ammonia. At a bulk NH_3/NH_4^+ ratio between 0 and approximately 1, at least five types of ammonium species may exist for samples 3 and 4. We assign the signal at $\delta = 6.9$ to ammonium ions located in a supercage, since this signal is also observed for sample 1 where the ammonium ions are located in the supercages only. The signals at $\delta = 6.5$ and 8.1 are assigned to ammonium ions located in the sodalite cages at cation sites II′ and I′, respectively. The line near $\delta = 6.9$ was already observed for different zeolites, but with a slightly different assignment.[16-21,27] The line at $\delta = 8.1$ is now reported for the first time.

Proton-Exchange of Ammonium Ions. Compared to the line at $\delta = 8.1$, the lines at $\delta = 6.5$ and $\delta = 6.9$ are shifted to higher field due to local proton exchange between an ammonia molecule and an acidic site. Clear indications for the existence of fast proton exchange comes from the experiments with excess loadings, which will be discussed further on (see the positions and areas of the "moving lines"). We note that for pyridine adsorption on acidic Y zeolites the lifetime of the pyridinium ions is 5×10^{-7} s at 313 K, which also implies fast exchange for this system.[42] Translational jumps of pyridinium ions occur after an average time of 10^{-5} s, which is also fast compared to the NMR experiment.[42] The signals observed in the region between $\delta = 6.9$ or 6.5 and $\delta = 8.1$ may then be assigned to fast exchange of ammonium ions between different cation positions. Since signals

due to ammonium ions and to the acidic protons are both observed in one spectrum, the process of exchange apparently does not involve the adsorption and desorption of ammonia at all acidic sites. This can be rationalized in the following way. While in part of the cages ammonia interacts with Brønsted sites under formation of ammonium species, Brønsted sites in other cages may be completely unaffected because diffusion of ammonia between these cages is slow. The local exchange process may involve translational motion of ammonium ions between sites I′ and II′ in the sodalite cages, but the occurrence of fast local proton exchange cannot be excluded with the present experiments. The residence time between two succeeding jumps is less than the typical time scale of the NMR experiment (less than approximately 1 ms). At high loadings, when all acidic sites are saturated, still a signal at $\delta = 6.5$ and a weak signal near $\delta = 8.1$ are observed for both samples 3 and 4, indicating that some of the ammonium ions in the sodalite cages do not participate in translational jumps. The translational jumps can only occur at low loadings, when only a few of the available cation positions in the cages are occupied.

Since at low loadings the main contribution to the ammonium species comes from the line at $\delta = 6.9$, we conclude that the produced ammonium ions are mainly located in the supercages. So, removal of the sodalite cage protons ($\delta = 4.6$) does not automatically result in sodalite cage ammonium ions. The protons at O_2 may react easily with ammonia and produce ammonium ions located in the supercages, e.g., at nearby cation sites II. When ammonia reacts with protons at sites O_3, the nearest cation sites for charge compensation may be sites of type III. Only in the presence of cesium ions, almost all of the ammonium ions are forced into the sodalite cages at site I′ ($\delta = 8.1$). At high loadings with ammonia on the other protic zeolites, we observe that some ammonium ions can be forced into the sodalite cages at site II′, without exchanging with other ammonium ions at site I′ or ammonia molecules in the supercages.

Freude and co-workers[20,21] reported that at high loadings fast exchange occurs predominantly between ammonium ions and ammonia molecules. This now determines the main features in the MAS NMR spectra (Figures 6–8). Two species can be discriminated. We observe a narrow signal, independent of the loading at $\delta = 5.3$ (samples 1–4) or $\delta = 5.9$ (sample 5). For the two dealuminated Y samples, this signal is observed at $\delta = 5.5$. From the observed positions we conclude that these signals are due to a complex, formed by two ammonium ions ($\delta = 8.1$) in fast exchange with one ammonia molecule ($\delta = 0.8$), which is located in the sodalite cage (resulting in the signal observed at $\delta = 5.9$). When such a species is located in the supercage, additionally fast exchange with acidic protons occurs and the line is shifted to $\delta = 5.3$. Since dealumination influences the position for this line, and since the position for this line also seems to correlate with the position of the lines for the acidic protons, whereas for the dealuminated sample the position of the ammonium line after partial reammoniation is observed at $\delta = 6.8$ (Table I), this also indicates that the exchange process involves the interaction of acidic protons with ammonia.

The second species mentioned above undergoes fast exchange with ammonia molecules and is the main signal in the NMR spectra at high loadings with ammonia. Proton transfer from ammonium ions to ammonia is the fastest step, and the chemical shift of this species is determined by the chemical shift of a non-exchanging ammonium ion, that of an ammonia molecule, and also by the total number of protons of the ammonium ions and the ammonia molecules. We will refer to this signal as the moving line. Ammonia in Na_{51}–Y gives rise to a signal at $\delta = 0.8$, independent of the amount adsorbed. The line width, as measured at room temperature at 300 MHz with a MAS frequency of 9 kHz, is 300 Hz at a loading of 5 ammonia molecules/unit cell and increases to 470 Hz at 26 ammonia molecules/unit cell (see Table II). For the low loading, increasing the temperature from 295 K to 320 K results in an increase of the line width, whereas at the high loading the line width is reduced. This is probably due to different sitings and exchange rates of the ammonia molecules at different loadings and temperatures. This results in differences in chemical shift (anisotropy), dipolar interactions, and mobilities. However, the limited temperature range used does not enable a more precise distinction.

TABLE II: Chemical Shifts of the "Moving Line" for the Different Samples at Different Loadings with Ammonia[a]

sample	NH_3/unit cell[b]	NH_3/NH_4^+[c] total	NH_3/NH_4^+[c] effective	δ (ppm) expt	δ (ppm) calc[d]	line width (Hz) 295 K	line width (Hz) 320 K
1	31	2.8	2.8	3.3	3.1 (2.8)	200	170
	51	5.4	5.4	2.5	2.3 (2.0)	90	100
2	51	0.8		4.9[e]			
	66	1.9	2.4	3.9	3.8 (3.3)	110	110
3	66	0.3	0.4	5.8	6.3 (5.4)	150	110
	87	0.7	1.1	4.9	4.8 (4.2)	60	60
	102	1.0	1.4	4.3	4.3 (3.8)	75	85
4	95	1.0	1.5	4.2	4.3 (3.7)	170	240
5	32	0.7	1.5	3.3	4.2 (3.6)	140	150
	64	2.6	3.9	2.2	2.7 (2.4)	100	170
6	5			0.8[f]		310	480
	26			0.8[f]		470	320

[a] Positions are in ppm and obtained from measurements at a field strength of 7.0 T and a MAS frequency of 9 kHz. [b] Number of ammonia molecules adsorbed. [c] Bulk and effective (only exchanging ammonium ions are taken into account) ratios obtained after adsorption. [d] Calculated chemical shift using $\delta = [1/(4n_{NH_4^+} + 3n_{NH_3})](4n_{NH_4^+}\delta_{NH_4^+} + 3n_{NH_3}\delta_{NH_3})$ with n representing the number of ammonium ions or ammonia molecules, $\delta_{NH_4^+} = 8.1$ (6.9) and $\delta_{NH_3} = 0.8$. [e] Strong overlap with intense line at $\delta = 5.2$. [f] No NH_4^+ present.

When increasing the loading with ammonia for the acidic zeolites up to approximately 100 molecules/unit cell, we observe a shift of a NMR signal to higher field (Figures 6–8). The position of the signal is partially determined by the ratio NH_3/NH_4^+ in the sample. For the same sample this line shifts to higher field, when the loading with ammonia is increased. However, the zeolite composition plays also an important role. Samples with similar bulk NH_3/NH_4^+ ratios show different chemical shifts for the moving line and *vice versa* (Table II). In the preceding part we already concluded that not all ammonium ions take part in the exchange process with the ammonia molecules present. Probably the local NH_3/NH_4^+ ratio determines the position of the moving line. When we calculate such an effective NH_3/NH_4^+ ratio, taking into account the number of ammonium ions, which do not exchange with almost all ammonia molecules ($\delta = 8.1$, 6.5, and also 5.3–5.9), we find a good agreement between the observed and the calculated chemical shifts for the samples 1–4, when using $\delta = 8.1$ for the chemical shift of a non–exchanging ammonium ion (see Table II). However, sample 5 shows a larger shift than expected from the calculations. This indicates that now exchange occurs via a more complicated process, which may involve the acidic sites.

From the above we can conclude that the chemical shift of non-exchanging or very slowly exchanging ammonium ions in zeolite Y is $\delta = 8.1$ in both types of cages. Since also ammonium ions are observed at higher field, we conclude that these species are exchanging with acidic sites. However, since both Brøsted sites and ammonium ions are observed in the same NMR spectrum, this exchange process does not involve all acidic sites. Probably, proton transfer is only from one ammonium ion to the nearest oxygen atoms and back. This local exchange, which involves only one or a few of the available acidic sites, is different from the mechanism used by Michel and co-workers,[29] where all adsorbed ammonia molecules are in equilibrium with all acidic sites. However, the latter mechanism seems to be valid for the moving line in the case of adsorption of excess ammonia. Differences in chemical shifts for the ammonium species ($\delta = 6.9$ and 6.5) may be due to structural differences (e.g., local

concentration of oxygen atoms or Brønsted sites) which affect the exchange process. The resulting chemical shift of the protons is determined by the lifetimes of the ammonium ion and its dissociated form (the ammonia molecule and the Brønsted site) and also by the chemical shifts of these species participating in the local equilibrium. The ammonium species at $\delta = 6.9$ are related to the hydroxyls at $\delta = 3.9$, while the ammonium species at $\delta = 6.5$ are related to the hydroxyls at $\delta = 4.6$. This implies a longer lifetime for the ammonium ions at $\delta = 6.9$ due to a higher acid strength of the Brønsted sites involved. Further, this implies that the line at $\delta = 8.1$ corresponds with non-exchanging or very slowly exchanging ammonium ions, in equilibrium with the most acidic protons. These ammonium ions are only observed in a large amount for cesium-exchanged sample 5 and in a considerably lower amount for highly exchanged samples 3 and 4. This result is in agreement with calorimetric measurements, where for completely exchanged Y zeolites a higher heat of adsorption for ammonia was observed than for Y zeolites with a degree of exchange of 85%.[43]

In the preceding part, differences in chemical shifts of the ammonium species were attributed to differences in proton exchange rates. Experiments over a more extended temperature interval are needed to confirm this suggestion. Differences in solvation by the zeolite walls at different cation sites may also influence the chemical shifts. Our results at high loadings with ammonia indicate, however, that the chemical shift of a very slowly exchanging or non-exchanging ammonium ion would be $\delta = 8.1$ in both supercages and sodalite cages. Further, the dealuminated samples indicate that differences in proton exchange rates dominate: the line at $\delta = 5.3$ is shifted to $\delta = 5.5$, corresponding with a higher acidity for the dealuminated sample. This shift cannot be explained by solvation effects, since we observe at low loadings the ammonium line at a similar position (even at a slightly lower value for δ) than for the nondealuminated samples.

Chemical Shift Dispersion, Dipolar Interactions. The line width of the moving line is influenced by the zeolite composition, amount of ammonia adsorbed and the temperature (see Table II). Generally, an increase of the loading with ammonia causes a decrease of the line width. However, for the completely exchanged sample at the highest loading applied, the line width has increased again. The temperature dependencies for samples 1 and 3 are similar over the range studied. At the highest loadings an increase in line width is observed, after the temperature is increased from 295 to 320 K. At lower loadings the reverse is observed. For sample 4 we observe for all loadings an increase of the line width for a similar increase in temperature. Clearly, there are different factors present which affect the line width of the moving line in a different way (e.g., differences in mobility and/or chemical shift dispersion). A similar conclusion was obtained for sample 6 loaded with ammonia. Since increasing the spinning rate from 3 to 9 kHz results in a decrease in line width by only a factor of 1–1.5, we can conclude that the main contribution to the line width (at 9-kHz spinning rate) comes from the dispersion of the isotropic chemical shift, similar to the situation found for the bridging hydroxyls.[22,23] There is, however, a measurable contribution from dipolar interactions at lower MAS speed.

The ^{1}H MAS NMR signals of the Brønsted sites give rise to strong spinning sidebands (Figure 9 and Table III). The strongest spinning sidebands are observed for sample 5, which contains mainly sodalite cage protons. However, this sample has also a slightly higher aluminium content. But, from the data in Table III (samples 3, 4, and 7) it is clear that the different spinning sideband intensity does not arise from a different aluminium content in sample 5. The difference is caused by a stronger ^{1}H–^{27}Al dipolar interaction, due to a shorter H–Al distance for the protons located in the sodalite cages. Fenzke and co-workers[25] found, from an analysis of the ^{1}H MAS NMR sideband patterns, for the H–Al distance a value of 0.248 nm for protons in the supercages and a value of 0.237 nm for protons in the sodalite cages. This difference may be due to the interaction of the sodalite cage acidic protons with the two close oxygen neighbors. This interaction weakens the O–H bond, which leads to the occurrence of a LF-OH band in the infrared spectrum. Because of the bond order conservation principle,[44] weakening of the O–H bond results in strengthening of the Si–O and Al–O bonds at the Brønsted site. So, this results in shorter Si–O and Al–O bonds and a longer O–H bond. The overall result of these changes is a shorter H–Al distance for the Brønsted sites in the sodalite cages.

TABLE III: Mean Sideband Intensities of the First Spinning Sidebands as Percentages of the Main Signals for MAS Frequencies of 3 and 6 kHz

		relative sideband intensity					
		Si–O^H–Al			NH_4^+		
sample	loading of NH_3/unit cell	δ	3 kHz	6 kHz	δ	3 kHz	6 kHz
1	0.0	3.9	44	13			
	3.6	3.9	47	12	6.9	8	2
2	0.0	3.9	47	13			
	3.6	3.9	46	13	6.9	12	4
	10.2	3.9	47	14	6.9	10	3
3	0.0	3.9	49	15			
	3.6	3.9	49	15	6.9	14	5
	10.2	3.9	49	15	6.9	14	4
4	0.0	3.9	51	15			
	3.9	3.9	51	15	6.9	19	6
	11.2	3.9	50	16	6.9	17	6
5	0.0	4.6	53	17			
	4.5	4.6	59	16	8.1	21	6
	9.7				8.1	21	6
7	0.0	4.0	49	15			
	3.0	4.0	48	15	6.8	12	4

When increasing the proton content of the zeolites (samples 1–3 in Table III), the relative intensities of the spinning sidebands for the Brønsted hydroxyls slightly increase. This is caused by the fact that the relative contribution of the sodalite cage protons to the peak height also increases.

At increasing but still low loadings the relative intensities of the spinning sidebands for the Brønsted hydroxyls and for the ammonium ions (Figures 9 and 10) both remain constant, which is in agreement with our previous conclusion that the adsorbing ammonia molecules show no preferences for specific acidic sites in a particular cavity. The spinning side bands of the ammonium ions (four protons) are of different origin than those for the Brønsted sites (one proton) and therefore not as strong (see Table 3).[27] In the case of low loading (not all acid sites have reacted) we observe the weakest spinning sidebands for the samples with the highest sodium content (samples 1 and 2). For sample 5, with the ammonium ions located at site I′, the strongest sidebands are observed. From Table III we see, that only a part of this increase in intensity may be attributed to differences in the Si/Al ratio or exchange degree. So we may conclude that these ammonium ions are more rigidly bonded. When excess ammonia is added, the sidebands decrease in intensity for all samples, presumably due to fast exchange between ammonium moieties with the mobile ammonia molecules. The spinning sidebands for the moving line are only very weak (a few percent or less at a spinning frequency of 3 kHz). The spinning sidebands of $\delta = 6.5$ and 5.3–5.9 are somewhat stronger (approximately 5–10% at 3 kHz). This order of sideband intensities is in agreement with the differences in fast exchange found for the different signals, resulting in the strongest spinning sidebands for the species with the highest ammonium character.

At low loadings the line widths of the NMR signals of the ammonium ions are sensitive to the MAS frequency (see Table IV). The changes in the line widths with increasing MAS frequency are determined by the composition of the sample (e.g., Na^+, H^+, NH_4^+) and the strength of the magnetic field. In a weaker field the influence of spinning is more pronounced. These

TABLE IV: Line Widths of the Ammonium Signals (δ = 6.9 and 8.1) Observed at Different Loadings on Different Zeolite Samples for Different MAS Frequencies

			line width (Hz) at 9.4 T 295 K and MAS			line width (Hz) at 7.0 T					
						295 K and MAS			320 K and MAS		
sample	loading of NH_3/unit cell	δ (ppm)	3 kHz	6 kHz	9 kHz	3 kHz	6 kHz	9 kHz	3 kHz	6 kHz	9 kHz
1	3.6	6.9	263	209	183	185	165	150	214	165	130
2	3.6	6.9	410	349	317						
	10.2	7.0	429	334	284	486	304	229	514	330	252
3	3.6	6.9	396	343	319	366	275	214	380	244	200
	10.2	6.9	388	317	279	381	260	219	397	259	205
4	3.9	7.0	489	434	403						
	11.2	7.0	491	424	388	388	338	303	409	320	264
5	4.5	8.1	438	380	343	387	343	305	357	270	230
	9.7	8.2	332	294	275						
7	3.0	6.8	356	310	287						

results indicate not only that chemical shift dispersion determines the line width but also that dipolar interactions are of importance. As for the Brønsted sites, differences in line widths for the ammonium signals may be due to different dipolar interactions and to differences in chemical shift dispersion. Since increasing the spinning rate from 3 to 9 kHz results in a reduction of the line width by only a factor 1–2, the main contribution to the line width is the isotropic chemical shift dispersion. At 320 K the effect of the MAS frequency is somewhat larger at very low loadings. Due to the temperature increase, the mobility of the ammonium ions has increased and the dipolar interactions are decreased.

At high loadings the observed bands are narrower (see the moving line in Table II) and less sensitive to the MAS frequency. This is due to the fast exchange between ammonium ions and highly mobile ammonia molecules (see above).

The influence of the temperature on the line width is probably rather complex. At a MAS frequency of 9 kHz increasing the temperature results in a reduced line width for all samples. However, since the effect of the MAS frequency depends also on temperature, we observe at 3 kHz and at very low loadings an increase of the line widths for ammonium ions in supercages (samples 1 and 2), while the line width for ammonium ions at site I′ in the sodalite cages (sample 5) decreases slightly (8%) with increasing temperature. So the ammonium ions in the sodalite cages at site I′ are more sensitive to temperature changes than the ions at other locations. Increasing the temperature probably results in an increased population of sites with higher mobility and hence results in an increase of the chemical shift dispersion. However, at the same time the dipolar interactions may be reduced. From our results we may conclude, that both effects are indeed operative. However, from the rather small influence of the spinning rate on the line widths we conclude that the main contribution comes again from the isotropic chemical shift dispersion.

Comparison with Earlier ^{15}N NMR Experiments. The results from our ^1H MAS NMR experiments can be compared with the result of ^{15}N CP MAS NMR experiments by Earl and coworkers.[30] When only a small amount of ammonia is adsorbed on the proton form of the Y zeolite, they observed a line at δ = −357 due to ammonium ions bonded to the lattice. This signal is probably related to the line we observe at δ = 6.9. When excess ammonia is adsorbed, lines near δ = −353, −358, −361, and −364 are observed. The line at δ = −353 is attributed to ammonium ions coordinated to the lattice. This line may be correlated with the weak line we observe near δ = 8.1. The other three features in the work of Earl were assigned to ammonium ions, which are hydrogen bonded to ammonia. We only observe two lines (δ = 5.3 and the moving line) for the species involving hydrogen bonding with ammonia. Since we observe for a comparable zeolite sample also a line at δ = 6.5, one of the weak lines at δ = −358 or −361 may correspond to this line in our spectrum, assigned to exchanging ammonium ions.

Conclusions

Room temperature adsorption of ammonia on zeolite Y shows that protons in supercages and sodalite cages react with this small strong base, without any preference for specific sites. Differences in acidity for Brønsted sites cannot be probed directly by room temperature adsorption of ammonia, since here the most important factor is the protonation of ammonia.

Adsorption of ammonia results in the formation of at least five NMR signals, depending on zeolite composition and loading with ammonia. Ammonium ions in the large supercages are observed at δ = 6.9 and ammonium ions in the small sodalite cages are observed at δ = 6.5 (site II′) and δ = 8.1 (site I′). At low loadings proton exchange between the ammonium ions with acidic sites in other cavities is slow on the time scale of the NMR experiment. But, proton transfer from an acidic site to a nearby ammonia molecule and back can be fast. In such a case a signal is observed with a chemical shift smaller than δ = 8.1, the value for a nonexchanging ammonium ion. Additionally to this fast exchange, fast translational jumps of ammonium ions to nearby cation sites may occur at low loadings, e.g., jumps between the sites I′ where local proton exchange is slow to sites II′ where local proton exchange is fast.

When an excess of ammonia is adsorbed onto the zeolite, a concentration dependent signal is found, indicating that proton exchange between ammonium ions and ammonia molecules is fast and proton exchange with Brønsted sites plays a negligible role. The position in the NMR spectrum of this line depends on the effective NH_3/NH_4^+ ratio (δ = 7 at low loadings and approaches δ = 1 at high loadings). At the same time, however, signals due to ammonium ions are still observed. So not all ammonium ions take part in the exchange processes. Further, clusters involving mainly fast exchange of two ammonium ions with one ammonia molecule can be observed at δ = 5.2–5.9. A small contribution to this signal comes from fast exchange involving these clusters and acidic hydroxyls.

After adsorption of small amounts of ammonia onto the acidic zeolite, the major part of the ammonium ions are located in the larger supercages. At high loadings with ammonia, and especially when large cesium ions are present in the supercages, the ammonium ions are forced into the smaller sodalite cages. For all species, except for the ammonium ions observed at δ = 8.1, proton exchange is fast on the time scale of the NMR experiment.

Finally, it has to be noted that the different ammonium species give rise to spinning sidebands of different intensities. The same holds for the different types of Brønsted sites, which give rise to even more intense spinning sidebands. So, for accurate quantitative studies of zeolite acidity by ammonia adsorption high MAS frequencies (9 kHz or more) should be used, at least at field strengths of 9.4 T or larger.

Acknowledgment. We are grateful to Drs. J.H.M.C. van Wolput for his assistance with the infrared measurements. Part

of this work was financially supported by the EEC (contract no. SC1-0199(GDF)).

References and Notes

(1) Rabo, J. A.; Gajda, G. J.; *Catal. Rev.*—Sci. Eng. **1989–90**, *31*, 85.
(2) Sauer, J. *J. Phys. Chem.* **1987**, *91*, 315.
(3) Mix, H.; Sauer, J.; Schröder, K.-P.; Merkel, A. *Collect. Czech. Chem. Commun.* **1988**, *53*, 2191.
(4) Sauer, J. *J. Mol. Catal.* **1989**, *54*, 312.
(5) Sauer, J. *Chem. Rev.* **1989**, *89*, 199.
(6) Teunissen, E. H.; Duijneveldt, F. B.; van Santen, R. A. *J. Phys. Chem.* **1992**, *96*, 366.
(7) Teunissen, E. H.; van Santen, R. A.; Jansen, A. P. J.; van Duijneveldt, F. B. *J. Phys. Chem.* **1993**, *97*, 203.
(8) Jacobs, P. A.; Uytterhoeven, J. B. *J. Chem. Soc., Faraday Trans. 1* **1973**, *69*, 359, 373.
(9) Uytterhoeven, J. B.; Christner, L. G.; Hall, W. K. *J. Phys. Chem.* **1965**, *69*, 2117.
(10) Ozin, G. A.; Baker, M. D.; Helwig, K.; Godber, J. *J. Phys. Chem.* **1985**, *89*, 1846.
(11) Baker, M. D.; Ozin, G. A.; Godber, J. *Catal. Rev.—Sci. Eng.* **1985**, *27*, 591.
(12) Ozin, G. A.; Baker, M. D.; Godber, J. *J. Phys. Chem.* **1989**, *93*, 2899.
(13) Jacobs, W. P. J. H.; van Santen, R. A.; Jobic, H. *J. Phys. Chem.*, submitted for publication.
(14) Udovic, T. J.; Cavanagh, R. R.; Rush, J. J.; Wax, M. J.; Stucky, G. D.; Jones, G. A.; Corbin, D. R. *J. Phys. Chem.* **1987**, *91*, 5968.
(15) Jacobs, W. P. J. H.; de Haan, V. O.; van Santen, R. A.; de Graaf, L. A. *J. Phys. Chem.*, submitted for publication.
(16) Freude, D.; Fröhlich, T.; Hunger, M.; Pfeifer, H.; Scheler, G. *Chem. Phys. Lett.* **1983**, *98*, 263.
(17) Freude, D.; Hunger, M.; Pfeifer, H.; Scheler, G.; Hoffman, J.; Schmitz, W. *Chem. Phys. Lett.* **1984**, *105*, 427.
(18) Pfeifer, H.; Freude, D.; Hunger, M. *Zeolites* **1985**, *5*, 274.
(19) Freude, D.; Hunger, M.; Pfeifer, H.; Schwieger, W. *Chem. Phys. Lett.* **1986**, *128*, 62.
(20) Freude, D.; Hunger, M.; Pfeifer, H.; *Z. Phys. Chem. (Munich)* **1987**, *152*, 171.
(21) Ernst, H.; Freude, D.; Hunger, M.; Pfeifer, H.; Seiffert, B. *Z. Phys. Chem. (Leipzig)* **1987**, *268*, 304.
(22) Brunner, E. *J. Chem. Soc., Faraday Trans.* **1990**, *86*, 3957.
(23) Brunner, E. *J. Chem. Soc., Faraday Trans.* **1993**, *89*, 165.
(24) Freude, D.; Klinowski, J. Hamdan, H. *Chem. Phys. Lett.* **1988**, *149*, 355.
(25) Fenzke, D.; Hunger, D.; Pfeifer, H. *J. Magn. Reson.* **1991**, *95*, 477.
(26) Hunger, M.; Freude, D.; Fenzke, D.; Pfeifer, H. *Chem. Phys. Lett.* **1992**, *191*, 391.
(27) Vega, A. J.; Luz, Z. *J. Phys. Chem.* **1987**, *91*, 365.
(28) Michel, D.; Germanus, A.; Scheller, D.; Thomas, B. *Z. Phys. Chem. (Leipzig)* **1981**, *262*, 113.
(29) Michel, D.; Germanus, A.; Pfeifer, H. *J. Chem. Soc., Faraday Trans. 1* **1982**, *78*, 237.
(30) Earl, W. L.; Fritz, P. O.; Gibson, A. A. V.; Lunsford, J. H. *J. Phys. Chem.* **1987**, *91*, 2091.
(31) Beyer, H. K.; Belenykaja, I. M. In *Proceedings of the International Symposium on Catalysis by Zeolites*, Villeurbanne, (Lyon), France, September 9–11, 1980; Imelik, B., Naccache, C., Ben Taarit, Y., Vedrine, J. C., Goudurier, G., Praliaud, H., Eds.; Elsevier; Amsterdam, 1980, Beyer, H. K.; Belenykaja, I. M. *Stud. Surf. Sci. Catal.* **1980**, *5*, 203.
(32) Beyer, H. K.; Belenykaja, I. M.; Hange, F.; Tielen, M., Grobet, P. J.; Jacobs, P. A. *J. Chem. Soc., Faraday Trans. 1* **1985**, *81*, 2889.
(33) Anderson, M. W.; Klinowski, J. *J. Chem. Soc., Faraday Trans. 1* **1986**, *82*, 1449.
(34) Kraushaar-Czarnetzki, B. Ph.D. Thesis, Eindhoven University of Technology, The Netherlands, 1989.
(35) Sherry, H. S. *J. Phys. Chem.* **1966**, *70*, 1158.
(36) Czjzek, M.; Jobic, H.; Fitch, A.; Vogt, T. *J. Phys. Chem.* **1992**, *96*, 1535.
(37) Jobic, H. Private communication.
(38) Jacobs, W. P. J. H.; Jobic, H.; van Wolput, J. H. M. C.; van Santen, R. A. *Zeolites* **1992**, *12*, 315.
(39) Hoffmann, J.; Hunger, B.; Streller, U.; Stock, Th.; Dombrowski, D.; Barth, A. *Zeolites* **1985**, *5*, 31.
(40) Jacobs, W. P. J. H.; van Wolput, J. H. M. C.; van Santen, R. A. *Zeolites* **1993**, *13*, 170.
(41) Maesen, Th. L. M. Ph.D. Thesis Delft University of Technology, The Netherlands, 1990.
(42) Rauscher, H.-J.; Michel, D.; Pfeifer, H. *J. Mol. Catal.* **1981**, *12*, 159.
(43) Jänchen, J. J. Unpublished results.
(44) van Santen, R. A. *Theoretical Heterogeneous Catalysis*; World Scientific: Singapore, 1991; pp 204, 320.